ELASTIC BUCKLING OF
LONGITUDINALLY STIFFENED PLATES UNDER SHEAR

by 683

KANG-SHYONG LIU

Diploma, Taipei Institute of Technology, 1962

A MASTER'S THESIS

submitted in partial fulfillment of the

requirements for the degree

MASTER OF SCIENCE

Department of Civil Engineering

KANSAS STATE UNIVERSITY

Manhattan, Kansas

1969

APPROVED BY:

Peter B. Cooper

Major Professor

TABLE OF CONTENTS

I. INTRODUCTION

The problem of elastic buckling of plates is often encountered in plate girder design as well as in airplane construction. In all cases of plate buckling, the critical values of normal or shearing forces are proportional to the flexural rigidity of the plate. Hence, the stability of the plate can always be increased by increasing its thickness. However, such a design will not normally be economical with respect to the weight of material used. A more economical solution is obtained by keeping the thickness of the plate as small as possible and increasing the stability by introducing reinforcing ribs. With this in mind, this research has presented an analytical analysis of the elastic buckling of stiffened plates.

As there are many cases of plate buckling, this study was limited in scope to rectangular plates of finite length, simply supported at the four edges and submitted to the action of uniformly distributed shearing stresses along the four edges. The plates are reinforced by a single longitudinal stiffener at various positions defined by the parameter η as shown in Fig. 1.

In analyzing the elastic buckling problem of a plate subjected to pure shear, the critical shearing stress τ_{cr} can be expressed as:

$$\tau_{cr} = k \frac{\pi^2 E}{12(1-\mu^2)} \frac{1}{\beta^2} \tag{1}$$

in which k is the plate buckling coefficient, E is the modulus of elas-

ticity, μ is Poisson's ratio and β is the web slenderness ratio. From the above equation it can be observed, in the case of constant β, that the critical shearing stress depends only on the buckling coefficient k. For a rectangular plate with one longitudinal stiffener, the values of k depend on α, the aspect ratio of the plate, η, the stiffener position parameter and γ^* the stiffener rigidity ratio. This research has determined the minimum stiffener rigidity ratio γ^* required to obtain the maximum buckling coefficient k_{max} for various values of α and η. Approximate design curves have also been prepared

II. REVIEW OF LITERATURE

In solving plate buckling problems, several methods have been developed. Among them, the differential equation method is the most exact one. However, since a solution using the differential equation is only possible in a few special cases, this theoretical method finds little use in practical work. There are three approximate methods[1] which are of interest and of practical use:

(i). Finite Difference Method

(ii). Statics Method

(iii). Energy Method

Although these three methods are approximate solutions to plate buckling problems, by using a high-speed digital computer the desired accuracy can be achieved within a reasonable amount of time.

In the early part of the 19th century, Navier and Saint-Venant derived the differential equations of a plate subjected to lateral loading and lateral loading combined with bending and tension or compression acting on the edges, respectively.[2,3] But, for the case of stiffened plates under shear, investigations have been completed only in the past 46 years (1921 - 1967).[4]

In 1921, Timoshenko published a paper on the stability of stiffened plates, which is notable not only because it represents one of the first on the subject, but also because the energy method was used for the first time to obtain approximate solutions to stability problems of stiffened plates.[4,5] With the assumption that the plate is homogenous and isotropic,

Southwell has also treated this problem extensively.[6] In 1929, Bergmann and Reissner extended Southwell's work to include the case of homogeneous and orthogonal-anisotropic plates with stiffeners of vanishing and comparatively low bending stiffness running longitudinally.[7] In 1930, Schmieden investigated the case of two or more longitudinal stiffeners having equal bending stiffness, but his data are confirmed only for the case of infinitely low bending stiffness.[8] In 1923, Huber established the theory and the general differential equation of bending in orthogonal-anisotropic plates.[9] Seven years later, Seydel applied his differential equation to solve the same structure subjected to shear.[10] In 1931, Timoshenko extended his own energy method from the case of one stiffener to two stiffeners.[3] In 1947, T. K. Wang extended Timoshenko's energy method to any number of stiffeners. Design curves also have been presented in Wang's paper.[11]

Recently, a series of papers by Klöppel and Scheer have treated a multitude of combinations of stiffener arrangements for simply supported rectangular plates.[12, 13] Based upon these papers, Klöppel and Scheer published a handbook in which various types of results based upon computer solutions have been shown in tables and charts.[1]

Most elastic buckling investigations of plates under shear have been done analytically. In the area of experimental work, Scott and Weber conducted a few tests in order to verify Timoshenko's theory.[14] Moore also reported on 60 different tests on aluminum-alloy 17S-T plats girders.[15]

III. METHOD OF ANALYSIS

1. Introduction

As mentioned above, there are three approximate methods for solving plate buckling problems that are of practical use. In this research the Rayleigh-Ritz energy method was used because it is the most convenient method for numerical calculation, especially using an electronic computer. Although the finite-difference method is also a powerful method for computer programming, for the case of stiffened plates one has to set up different simultaneous equations for different parameters. With the Rayleigh-Ritz method the buckling matrices can be set up for a general case and directly utilized for chosen values of the parameters. In 1960, Kloppel and Scheer published a handbook which presents tables and charts covering a large number of elastic stability problems for stiffened, simply-supported, rectangular plates.[1] These tables and charts were obtained using the energy method, and a digital computer was utilized to solve the buckling matrices for the various problems. However, in this handbook, the minimum stiffener rigidity ratio γ^* was not given for any of the cases considered. Also, two simple approximate formulae, i.e.,

$$k_{max} = \{4.00 + 5.34/[\alpha/(1-\eta)]^2\}/(1-\eta)^2, \quad \text{for } \alpha/(1-\eta) \leq 1 \tag{2}$$

$$k_{max} = \{5.34 + 4.00/[\alpha/(1-\eta)^2]\}/(1-\eta)^2 \quad \text{for } \alpha/(1-\eta) \geq 1 \tag{3}$$

were employed to calculate the upper limiting buckling values for the case of a rectangular plate with one longitudinal stiffener subjected to pure shear. In this research, the limiting buckling values were calculated by a more exact method. In addition, the curves for the minimum stiffener rigidity ratio γ^* are also presented for different plate aspect ratios and position parameters. Simple cubic polynomial equations have also been obtained to fit those curves for practical design purposes.

In general the Rayleigh-Ritz[17] method is obtained in the following steps: first, assume the solution in the form of a series which satisfies the boundary conditions but with undetermined parameters A_m; second, insert these functions into the expression for the potential energy or the complementary energy, and carry out any required integration. The resulting expressions are functions of the undetermined parameters A_m, where m = 1, 2, ... Since the potential energy or the complementary energy must be a minimum for equilibrium, these parameters can be determined from the minimizing conditions

$$\frac{\partial \pi}{\partial A_1} = 0, \quad \frac{\partial \pi}{\partial A_2} = 0, \ . \ . \ . \qquad \text{or}$$

$$\frac{\partial \pi^*}{\partial A_1} = 0, \quad \frac{\partial \pi^*}{\partial A_2} = 0, \ . \ . \ . \tag{4}$$

in which π is the total potential energy and π^* is the correspondent complementary energy. If m parameters are taken, Eq. 4 gives m

simultaneous equations from which these parameters may be solved. In this investigation, a double Fourier series

$$w(x,y) = \sum_m \sum_n A_{mn} \text{ SIN } \frac{m\pi x}{a} \text{ SIN } \frac{n\pi y}{b} \tag{5}$$

was assumed to represent the deflection surface of the plate in the z direction. The potential energy of the plate was calculated from this assumed function. In Eq. 5, A_{mn} are the undetermined parameters, where $m = 1, 2, \ldots, n = 1, 2, \ldots$, and a and b are the dimensions of the plate in the x and y directions, respectively. Since this investigation deals with the elastic buckling of the plate, the minimizing conditions of the derivatives of the total potential energy based on Eq. 5 give m x n homogeneous linear equations form a buckling matrix [M] of m x n order. For the sake of easy computation of the smallest eigenvalue, that is, the dimensionless buckling coefficient k, of the matrix [M], the matrix [M] is separated into two matrices [A] and k[B]. Eventually, the following matrix equation will be obtained:

$$[A] = k[B] \tag{6}$$

in which both [A] and [B] are square matrices of m x n order. Solution of Eq. 6 will yield k values for different η and α values.

2. Assumptions

The following assumptions were used in this investigation:

1. Hooke's law is valid.
2. The plate is homogeneous and isotropic.
3. Boundary stresses are uniformly distributed.
4. Any stretching in the middle plane of the plate is negligible.
5. The deflections of the plate are small.

3. Derivation of the Governing Matrix Equation

The following energy equations will be employed to derive the governing matrix equation:[3]

(1) Internal energy of the plate.

$$U_p = \frac{D}{2} \iint \{ \left(\frac{\partial^2 w}{\partial x^2} + \frac{\partial^2 w}{\partial y^2} \right)^2 - 2(1-\mu) \left[\frac{\partial^2 w}{\partial x^2} \frac{\partial^2 w}{\partial y^2} - \left(\frac{\partial^2 w}{\partial x \partial y} \right)^2 \right] \} \, dxdy \quad (7)$$

(2) Internal energy of the stiffener

$$U_s = \frac{EI_s}{2} \int \left(\frac{\partial^2 w}{\partial x^2} \right)^2_{(y=\eta \cdot b)} \cdot dx \quad (8)$$

(3) External energy of the plate

$$W = t \cdot \tau \iint \frac{\partial w}{\partial x} \frac{\partial w}{\partial y} \, dxdy \quad (9)$$

(4) Total potential energy

$$= U_p + U_s - W \quad (10)$$

The derivation of the governing matrix equation can be carried out

in the following steps:

1. Calculation of derivatives

$$w(x,y) = \sum_m \sum_n A_{mn} \text{ SIN } \frac{m\pi x}{a} \text{ SIN } \frac{n\pi y}{b} \tag{11}$$

$$\frac{\partial w}{\partial x} = + \sum_m \sum_n \frac{m\pi}{a} A_{mn} \text{ COS } \frac{m\pi x}{a} \text{ SIN } \frac{n\pi y}{b} \tag{12}$$

$$\frac{\partial w}{\partial y} = + \sum_m \sum_n \frac{n\pi}{b} A_{mn} \text{ SIN } \frac{m\pi x}{a} \text{ COS } \frac{n\pi y}{b} \tag{13}$$

$$\frac{\partial^2 w}{\partial x^2} = - \sum_m \sum_n \frac{m^2\pi^2}{a^2} A_{mn} \text{ SIN } \frac{m\pi x}{a} \text{ SIN } \frac{n\pi y}{b} \tag{14}$$

$$\frac{\partial^2 w}{\partial y^2} = - \sum_m \sum_n \frac{n^2\pi^2}{b^2} A_{mn} \text{ SIN } \frac{m\pi x}{a} \text{ SIN } \frac{n\pi y}{b} \tag{15}$$

$$\frac{\partial^2 w}{\partial x \partial y} = + \sum_m \sum_n \frac{mn\pi^2}{ab} A_{mn} \text{ COS } \frac{m\pi x}{a} \text{ COS } \frac{n\pi y}{b} \tag{16}$$

2. Orthogonal relationship of the assumed double Fourier series

$$\int_0^a \text{SIN } \frac{m\pi x}{a} \text{ SIN } \frac{p\pi x}{a} \, dx \begin{cases} = 0 \text{ for } m \neq p \\ = \frac{a}{2} \text{ for } m = p \end{cases} \tag{17}$$

$$\int_0^a \text{COS } \frac{m\pi x}{a} \text{ COS } \frac{p\pi x}{a} \, dx \begin{cases} = 0 \text{ for } m \neq p \\ = \frac{a}{2} \text{ for } m = p \end{cases} \tag{18}$$

$$\int_0^a \text{SIN}\,\frac{m\pi x}{a}\ \text{COS}\,\frac{p\pi x}{a}\,dx\ \begin{cases} = 0 & \text{for } m+p = \text{even} \\ = \dfrac{2a}{\pi}\cdot\dfrac{m}{m^2-p^2} & \text{for } m+p = \text{odd} \end{cases} \tag{19}$$

3. Calculation of the internal energy of the plate, U_p and $\frac{\partial U_p}{\partial A_{mn}} \cdot C$

$$U_p = \frac{D}{2}\int_0^a\int_0^b \{(\frac{\partial^2 w}{\partial x^2}+\frac{\partial^2 w}{\partial y^2})^2 - 2(1-\mu)\ [\frac{\partial^2 w}{\partial x^2}\frac{\partial^2 w}{\partial y^2} - (\frac{\partial^2 w}{\partial x \partial y})^2]\,dxdy \tag{20}$$

Substituting w and its derivatives from Eqs. 11, 14, 15 and 16 into Eq. 20, it can be shown that the integral of the terms in the brackets vanishes:

$$\int_0^a\int_0^b 2(1-\mu)\ \sum_m\sum_n\sum_p\sum_q \{\frac{m^2q^2\pi^4}{a^2b^2}\cdot A_{mn}\,A_{pq}\cdot \text{SIN}\,\frac{m\pi x}{a}\cdot \text{SIN}\,\frac{n\pi y}{b}$$

$$\cdot\ \text{SIN}\,\frac{p\pi x}{a}\cdot \text{SIN}\,\frac{q\pi y}{b} - \frac{mnpq\pi^4}{a^2b^2}A_{mn}\cdot A_{pq}\cdot \text{COS}\,\frac{m\pi x}{a}$$

$$\text{COS}\,\frac{n\pi y}{b}\cdot \text{COS}\,\frac{p\pi x}{a}\cdot \text{COS}\,\frac{q\pi y}{b}\}dxdy$$

$$= \sum_m\sum_n 2(1-\mu)\ (\frac{m^2n^2\pi^4}{a^2b^2} - \frac{m^2n^2\pi^4}{a^2b^2})\,\frac{a}{2}\cdot\frac{b}{2}A_{mn}^2 = 0 \tag{21}$$

So, Eq. 22 is obtained,

$$U_p = \frac{D}{2}\cdot\frac{\pi^4}{a^4}\cdot\frac{a}{2}\cdot\frac{b}{2}\sum_m\sum_n A_{mn}^2\,(m^2+\alpha^2n^2)^2$$

$$= \sigma_e \cdot \frac{\pi^2}{8} \cdot \frac{t}{\alpha 3} \cdot \sum_m \sum_n A_{mn}^2 \, (m^2 + \alpha^2 n^2)^2 \tag{22}$$

in which

$$\sigma_e = \frac{\pi^2 \cdot E \cdot t^2}{12 \cdot b^2 \cdot (1-\mu^2)} \tag{23}$$

and

$$\frac{\partial U_p}{A_{mn}} = \frac{\sigma_e \pi^2 t}{4\alpha^3} \cdot A_{mn} \, (m^2 + \alpha^2 n^2)^2 \tag{24}$$

To simplify setting up the matrix equation, $\frac{\partial U_p}{\partial A_{mn}}$ is multiplied by a constant C ($C = \frac{4\alpha^3}{t\pi^2 \cdot \sigma_e} = \frac{4a^3}{b \cdot \pi^4 \cdot D}$). So,

$$\frac{\partial U_p}{\partial A_{mn}} \cdot C = \frac{4\alpha^3}{t\pi^2 \sigma_e} \cdot \frac{\sigma_e \cdot \pi^2 \cdot t}{4\alpha^3} \cdot A_{mn} (m^2 + \alpha^2 n^2)^2 = A_{mn} \cdot R_{mn} \tag{25}$$

in which $R_{mn} = (m^2 + \alpha^2 n^2)$ (26)

4. Calculation of the internal energy of the stiffener U_s and $\frac{\partial U_s}{\partial A_{mn}} \cdot C$

$$U_s = \frac{EI_s}{2} \int_o^a \left(\frac{\partial^2 w}{\partial x^2} \right)^2_{(y=\eta \cdot b)} \cdot dx$$

$$= \frac{EI_s}{2} \cdot \frac{\pi^4}{a^4} \int_o^a \sum_m \sum_n \sum_p \sum_q A_{mn} A_{pq} \, m^2 p^2 \, \text{SIN} \frac{m\pi x}{a}$$

$$\text{SIN } \frac{p\pi x}{a} \cdot \text{SIN } n\pi\eta \cdot \text{SIN } q\pi\eta\} \, dx$$

$$= \frac{EI_s}{2} \cdot \frac{\pi^4}{a^4} \cdot \frac{a}{2} \sum_m \sum_n \sum_q m^4 A_{mn} A_{mq} \text{ SIN } n\pi\eta \cdot \text{SIN } q\pi\eta$$

$$= \gamma_L \cdot \sigma_e \cdot \pi^2 \cdot \frac{t}{4} \cdot \frac{1}{a^3} \sum_m \sum_n \sum_q m^4 A_{mn} A_{mq} \text{ SIN } n\pi\eta$$

$$\cdot \text{SIN } q\pi\eta \qquad (27)$$

Multiplying the derivative of U_s with respect to A_{mn} with C,

$$\frac{\partial U_s}{\partial A_{mn}} \cdot C = \frac{4a^3}{t\pi^2\sigma_e} \gamma_L \cdot \sigma_e \cdot \pi^2 \cdot \frac{t}{2} \cdot \frac{m^4}{a^3} \text{ SIN } n\pi\eta$$

$$\sum_q A_{mq} \cdot \text{SIN } q\pi\eta$$

$$= 2m^4 \cdot \gamma_L \cdot \text{SIN } n\pi\eta \sum_q A_{mq} \text{ SIN } q\pi\eta$$

$$= S_m \cdot \text{SIN } n\pi\eta \sum_q A_{mq} \text{ SIN } q\pi\eta \qquad (28)$$

in which

$$S_m = 2 \cdot m^4 \cdot \gamma_L \qquad (29)$$

5. Calculation of the external energy of the plate W and $\frac{\partial W}{\partial A_{mn}} \cdot C$

$$W = + t \cdot \tau \int_o^a \int_o^b \frac{\partial w}{\partial x} \frac{\partial w}{\partial y} \, dxdy$$

$$= + t \cdot \tau \cdot \frac{\pi^2}{a \cdot b} \int_o^a \int_o^b \{ \sum_m \sum_n \sum_p \sum_q m \cdot q \cdot A_{mn} \cdot A_{pq}$$

$$\cos \frac{m\pi x}{a} \cdot \sin \frac{p\pi x}{a} \cdot \sin \frac{n\pi y}{b} \cdot \cos \frac{q\pi y}{b} \} \, dxdy$$

$$= + t \cdot \tau \cdot \frac{\pi^2}{a \cdot b} \frac{4a \cdot b}{\pi^2} \sum_m \sum_n \sum_p \sum_q A_{mn} \cdot A_{pq} \frac{mnpq}{(p^2 - m^2)(n^2 - q^2)}$$

$$= - 4t \cdot \tau \cdot \sum_m \sum_n \sum_p \sum_q A_{mn} \cdot A_{pq} \frac{mnpq}{(m^2 - p^2)(n^2 - q^2)} \qquad (30)$$

$$\left(\begin{matrix} m + p \\ n + q \end{matrix} \right\} = \text{odd})$$

The derivative of W with respect to A_{mn} is as follows:

$$\frac{\partial W}{\partial A_{mn}} \cdot C = - 8t \cdot \tau \sum_p \sum_q A_{pq} \cdot \frac{mnpq}{(m^2 - p^2)(n^2 - q^2)} \qquad (31)$$

$$\left(\begin{matrix} m + p \\ n + q \end{matrix} \right\} = \text{odd})$$

Multiplying $\frac{\partial W}{\partial A_{mn}}$ by C,

$$\frac{\partial W}{\partial A_{mn}} \cdot C = -\frac{4\alpha^3}{t\pi^2\sigma_e} \cdot 8t \cdot \tau \cdot \sum_p \sum_q A_{pq} \frac{mnpq}{(m^2-p^2)(n^2-q^2)}$$

$$= -T \cdot k \sum_p \sum_q A_{pq} \frac{mnpq}{(m^2-p^2)(n^2-q^2)} \qquad (32)$$

$$\begin{pmatrix} m+p \\ n+q \end{pmatrix} = \text{odd}$$

in which

$$T = \frac{32\alpha^3}{\pi 2} \qquad (33)$$

6. Calculation of the total energy Π

$$\Pi = U_p + U_s - W$$

$$= \sigma_e \cdot \frac{\pi^2}{8} \cdot \frac{t}{\alpha^3} \sum_m \sum_n A_{mn}^2 (m^2 + \alpha^2 n^2)^2$$

$$+ \gamma_L \sigma_e \pi^2 \cdot \frac{t}{A} \cdot \frac{1}{\alpha^3} \sum_m \sum_n \sum_q m^4 A_{mn} A_{mq} \text{ SIN } n\pi\eta \cdot \text{SIN } q\pi\eta$$

$$+ 4 \cdot t \cdot \tau \cdot \sum_m \sum_n \sum_p \sum_q A_{mn} A_{pq} \frac{mnpq}{(m^2-p^2)(n^2-q^2)} \qquad (34)$$

7. Calculation of $\frac{\partial \Pi}{\partial A_{mn}} \cdot C$

$$\frac{\partial \Pi}{\partial A_{mn}} \cdot C = \frac{\partial U_p}{\partial A_{mn}} \cdot C + \frac{\partial U_s}{\partial A_{mn}} \cdot C - \frac{\partial W}{\partial A_{mn}} \cdot C$$

$$= A_{mn} \cdot R_{mn} + S_m \cdot \text{SIN } n\pi\eta \sum_q A_{mq} \text{ SIN } q\pi\eta$$

$$+ T \cdot k \cdot \sum_p \sum_q A_{pq} \frac{mnpq}{(m^2-p^2)(n^2-q^2)} \tag{35}$$

8. Setting $\frac{\partial \Pi}{\partial A_{mn}} \cdot C$ equal to zero

$$A_{mn} \cdot R_{mn} + S_m \cdot \text{SIN } n\pi\eta \sum_q A'_{mq} \text{ SIN } q\pi\eta$$

$$+ T \cdot k \cdot \sum_p \sum_q \frac{mnpq}{(m^2-p^2)(n^2-q^2)} = 0 \tag{36}$$

or

$$A_{mn} \cdot R_{mn} + S_m \cdot \text{SIN } n\pi\eta \sum_q A_{mq} \text{ SIN } q\pi\eta$$

$$= -k \cdot T \cdot \sum_p \sum_q A_{pq} \frac{mnpq}{(m^2-p^2)(n^2-q^2)} \tag{37}$$

9. Setting up the buckling matrix

Choosing different values A_{11}, A_{12}, ... A_{mn} in Eq. 37, the following matrix equation is obtained:

$$[A][X] = k[B][X] \tag{38}$$

in which both [A] and [B] are symmetrical matrices of m x n order, [X] is a column matrix of independent variables known as the eigenvector.

4. Solution of the Matrix Equation

The buckling coefficient k in Eq. 38 is, mathematically, the smallest eigenvalue of that matrix equation. There are many numerical approaches[18,19] to the solution of Eq. 38. The successive rotation method[19] was used in this investigation. This method requires the transformation of Eq. 38 into the form

$$[Q][Z] = k[Z] \tag{39}$$

in which k is the eigenvalue of [Q] and [Z] is the eigenvector corresponding to that specific eigenvalue, [Q] is a new matrix derived from [A] and [B]. The method also requires that [Q] be a symmetrical matrix after the transformation. Then, successive rotation transformation are applied to both sides of Eq. 39, until $[Q_m]$ is obtained such that all nondiagonal terms are zero. The diagonal terms of this $[Q_m]$ will then

be equal to the eigenvalues and the smallest one (absolute values considered only) is the buckling coefficient sought.

Eq. 39 can be obtained according to the following steps:

1. Examine the positive definiteness of matrices [A] and [B] of Eq. 38[20]. If both [A] and [B] are positive definite or only [B] is positive definite, Eq. 38 can be used directly to obtain Eq. 39. If neither [A] nor [B] is positive definite, there is no guarantee that a real solution of eigenvalues exists. If only [A] is positive definite, Eq. 38 should be arranged in the form

$$[B][x] = \frac{1}{k}\,[A][x] \tag{40}$$

For the case of a stiffened plate subjected to pure shear, [B] is always not positive definite. Therefore Eq. 40 will be used to derive Eq. 39

2. Diagonalize [A]

[A] can be diagonalized by introducing a sequence of squares matrices $[T_r]$ and operating as follows,

$$\begin{aligned}
[A] &= [A_o] \\
[T_1]'\,[A_o]\,[T_1] &= [A_1] \\
[T_2]'\,[A_1]\,[T_2] &= [A_2] \\
&\cdots\cdots\cdots \\
[T_r]'\,[A_{r-1}]\,[T_r] &= [A_r] \\
&\cdots\cdots\cdots
\end{aligned} \tag{41}$$

so that

$$[T_r]' \ldots [T_2]'[T_1]'[A][T_1][T_2] \ldots [T_r] = [A_r] \tag{42}$$

in Eqs. 41 and 42, $[T_r]$ is a rotation matrix

$$[T_r] = \begin{array}{c} \\ \\ \\ \\ \\ \\ \\ \\ \end{array} \begin{array}{c} \begin{array}{cccccccccccc} & & & & & & p & & q & & & \end{array} \\ \begin{bmatrix} 1 & 0 & \cdot & \cdot & \cdot & 0 & 0 & 0 & 0 & \cdot & \cdot & \cdot & 0 \\ 0 & 1 & \cdot & \cdot & \cdot & 0 & 0 & 0 & 0 & \cdot & \cdot & \cdot & 0 \\ \cdot & \cdot & \cdot & \cdot & \cdot & \cdot & \cdot & \cdot & \cdot & \cdot & \cdot & \cdot & \cdot \\ 0 & 0 & \cdot & \cdot & \cdot & C & 0 & 0 & -S & \cdot & \cdot & \cdot & 0 \\ 0 & 0 & \cdot & \cdot & \cdot & 0 & 1 & 0 & 0 & \cdot & \cdot & \cdot & 0 \\ 0 & 0 & \cdot & \cdot & \cdot & 0 & 0 & 1 & 0 & \cdot & \cdot & \cdot & 0 \\ 0 & 0 & \cdot & \cdot & \cdot & S & 0 & 0 & C & \cdot & \cdot & \cdot & 0 \\ \cdot & \cdot & \cdot & \cdot & \cdot & \cdot & \cdot & \cdot & \cdot & \cdot & \cdot & \cdot & \cdot \\ 0 & 0 & \cdot & \cdot & \cdot & 0 & 0 & 0 & 0 & \cdot & \cdot & \cdot & 1 \end{bmatrix} \end{array} \tag{43}$$

where C = COSθ and S = SINθ. The rotation matrix is employed such that each $[T_r]$ causes a particular off-diagonal element a_{pq} in $[A_r]$ to vanish. As $[T_r]$ is an orthogonal matrix, the transpose of $[T_r]$ is equal to its inverse

$$[T_r]' = [T_r]^{-1} \tag{44}$$

It can be shown also that the product of any two orthogonal matrices

remains orthogonal. Therefore, if we let

$$[V] = [T_1][T_2] \ldots [T_r] \tag{45}$$

we obtain

$$[V]^{-1} = [V]' = \{[T_1][T_2] \ldots [T_r]\}' = [T_r]' \ldots [T_2]'[T_1]' \tag{46}$$

So Eq. 42 becomes

$$[V]'[A][V] = [A_r] \tag{47}$$

and

$$[V][V]'[A][V][V]' = [V][A_r][V]' \tag{48}$$

or

$$[A] = [V][A_r][V]' \tag{49}$$

Letting

$$[D] = [A_r],$$

Eq. 49 becomes

$$[A] = [V][D][V]' \tag{50}$$

3. Substitute Eq. 50 into Eq. 40

$$[B][x] = \frac{1}{k}[V][D][V]'[x] \tag{51}$$

4. Premultiply both sides of Eq. 51 by [V]'

$$[V]'[B][x] = \frac{1}{k}[D][V]'[x] \tag{52}$$

5. Define [H] = [V]'[B][V] and [Y] = [V]'[x].

Eq. 53 takes the form

$$[H][Y] = \frac{1}{k}[D][Y] \tag{54}$$

5. Take the square root of [D]

As [A] is assumed to be positive definite, every element of the diagonal matrix [D] is real and positive. In other words, [D] can be taken as

$$[D] = [G][G] \tag{55}$$

in which $g_{ii} = \sqrt{d_{ii}}$ (56)

such that

$$[H][Y] = \frac{1}{k}[G][G][Y] \tag{57}$$

or

$$[G]^{-1}[H][G]^{-1}[G][Y] = \frac{1}{k}[G][Y] \tag{58}$$

6. Let $[G]^{-1}[H][G]^{-1} = [Q]$ and

$$[G][Y] = [Z].$$

Equation 58 becomes

$$[Q][Z] = \frac{1}{k}[Z] \tag{59}$$

7. Diagonalize [Q].

The technique described in step 2 can be employed to diagonalize [Q]. The final result becomes

$$[Q] = [S][K][S]' \tag{60}$$

in which [S] is a square matrix of n eigenvectors assembled together, [K] is of the form

$$\begin{bmatrix} 1/k_1 & 0 & 0 & 0 & 0 & 0 \\ 0 & 1/k_2 & 0 & 0 & 0 & 0 \\ 0 & 0 & 1/k_3 & 0 & 0 & 0 \\ 0 & 0 & 0 & . & 0 & 0 \\ . & . & . & . & . & . \\ 0 & 0 & 0 & 0 & 0 & 1/k_n \end{bmatrix}$$

$1/k_1$, $1/k_2$, . . . $1/k_n$ are eigenvalues of [Q]. The buckling coefficient k is k_i in Eq. 61 that has the smallest absolute value.

5. Programming the Problem for Computer Solution

Though all buckling coefficients in this research were calculated by high-speed IBM 360/system computer, for the sake of generality the FORTRAN IV program is not presented in this thesis. Instead, a complete flow diagram has been developed in Appendix I. The steps of this flow diagram simply follow the numerical procedures derived in the previous section.

IV. SELECTION OF THE SERIES COMPONENTS AND ACCURACY

As introduced in Section III, the estimated approximation

$$w(x,y) = \sum_m \sum_n A_{mn} \cdot \text{SIN} \frac{m\pi x}{a} \cdot \text{SIN} \frac{n\pi y}{b} \qquad (62)$$

was assumed to solve the buckling coefficient problem. For a very rigorous solution, the two summations over m and n would have to be taken from 1 to ∞; from this a matrix of infinite order would result. Although an exact solution is not available from Eq. 62, through correct selection of the series components, sufficiently accurate buckling coefficients, which deviate at most around 2% from the exact solution, can be obtained. From extensive calculations by Borsch-Supan[21,22] and based on preliminary work in this investigation, the choice of the components should be as follows:

1. For plates with a symmetrical stiffener arrangement, both m and n vary from 1 to 6.
2. For plates with $\alpha < 3$ and without a symmetrical stiffener arrangement, m = 1 to 5.
3. For plates without a stiffener, the choice of the components varies greatly. In general, m = 1 to 5, n = 1 to 6 for $0.5 < \alpha < 1$, and m = 1 to 7, n = 1 to 5 for $1 \leq \alpha \leq 6$.

V. RESULTS AND DISCUSSION

1. Limiting Buckling Values

The limiting buckling values (upper limits) are the buckling values related to the "Euler" buckling stress of the whole plate. When the stiffened plate (Fig. 1) is subjected to shearing stresses, if the rigidity of the stiffener is not large enough, the inclined waves of the buckled plate run across the stiffener and buckling of the plate is accompanied by bending of the stiffener. By subsequent increase of the rigidity of the stiffener, a condition in which each part of the plate will buckle as a rectangular plate with simply supported edges and the stiffener will remain straight, may be finally achieved. The upper limits of the buckling coefficients are those corresponding to the limiting buckling values.

Theoretically, the above-mentioned limiting buckling values are not the maximum buckling values attainable. If the rigidity of the stiffener is increased beyond the point where the plate obtains its limiting buckling value, greater buckling values can be obtained. However, because of the following two conditions the limiting buckling values have been referred to as maximum buckling coefficients throughout this research:

(1) The possible increase of k above the limiting buckling value only extends from 0 to 15%, however the corresponding required increase in the rigidity of stiffener is much higher than that required below the limiting buckling values.

(2) The dimensions of the matrices would be enormously large in

order to have sufficiently exact values above the limiting buckling values.

As the limiting buckling values can be calculated by assuming that each part of the stiffened plate buckles as a rectangular plate with simply supported edges, some buckling values for unstiffened plates are needed first to calculate these limiting buckling values. These buckling values for unstiffened plates k_u are tabulated in Table 1 for values of α ranging from 0.625 to 6.0. The corresponding stiffened plates are also listed in the table.

From the buckling coefficients listed in Table 1, the limiting buckling values for the corresponding stiffened plates k_{max} can easily be calculated by the following equation:

$$k_{max} = k_u/(1-\eta)^2 \tag{65}$$

The results of this calculation are presented in Table 2. For comparison, approximate values obtained using Eqs. 2 and 3 are also included in Table 2. For design purposes, the more exact values based on the Rayleigh-Ritz method have also been presented in graphical form in Fig. 3.

From Fig. 2, it can be observed that there are some discontinuities in the curves, e.g. at $\alpha = 1.6, 2.8$, for $\eta = 0.2$; $\alpha = 1.26, 2.1, 3.0$ for $\eta = 0.4$; etc. This phenomenon can be explained as follows: the limiting buckling values were calculated by a matrix of (m x n) x (m x n) dimensions, in which m and n are components of the assumed double Fourier's series, for the unstiffened plate. Because of the symmetry of the plate,

the matrix can be split into two independent matrices, one for m + n = even and the other for m + n = odd. Calculations show that the two matrices give the critical values alternately. The discontinuities are transition points from one group to another group of matrices.

2. Charts of Minimum Rigidity Ratio vs. Plate Aspect Ratio

Following the procedures of the flow diagram in Appendix I and using the limiting buckling values of Table 2, the minimum required rigidity ratio γ^* (EI_s/bD) for maximum buckling coefficients have been calculated for η = 0.2, 0.3, 0.4 and 0.5. The results are presented graphically for α ranging from 0.5 to 3.0, in Figs. 4, 5, 6 and 7.

3. Use of the Charts

Although the minimum required rigidity ratio γ^* has been calculated only for η = 0.2, 0.3, 0.4 and 0.5, the charts presented in Figs. 4, 5, 6 and 7 can be used to advantage in the following two ways:

(1) Apply the polynomial interpolation method to obtain the desired γ^* values. A flow diagram for the computer solution of this method is presented in Appendix III.

(2) Follow the procedures of the flow diagram of Appendix I to find γ^* values by computer and check some points with the charts. If smaller matrix dimensions are used, determine the factor of deviation. Then, approximate results can be obtained by multiplying each answer with the factor of deviation. For γ^* values between α = 0 and α = 0.5, a linear variation

between the origin and the calculated value of γ^* at $\alpha = 0.5$ gives satisfactory values.

4. Approximate Design Equations

It was observed that the curves in Figs. 4 through 7 have some common characteristics. Considering a curve as shown in Fig. 2, it is obvious that each section of the curve as indicated in the figure represents the corresponding curve in Figs. 4 through 7. With this in mind, a curve-fitting process has been carried out by the method of Least Square. As there is one inflection point to each curve, a cubic function was assumed. The results were as follows:

$$\gamma^*_{\eta = 0.2} = 22.4 - 79.3\alpha + 81.5\alpha^2 - 18.9\alpha^3 , \quad \text{for } 0.5 \leq \alpha \leq 2.0 \tag{66}$$

$$\gamma^*_{\eta = 0.3} = 23.5 - 86.8\alpha + 93.4\alpha^2 - 20.6\alpha^3 , \quad \text{for } 0.5 \leq \alpha \leq 2.5 \tag{67}$$

$$\gamma^*_{\eta = 0.4} = 13.3 - 57.0\alpha + 72.1\alpha^2 - 13.7\alpha^3 , \quad \text{for } 0.5 \leq \alpha \leq 3.0 \tag{68}$$

$$\gamma^*_{\eta = 0.5} = 27.7 - 142.7\alpha + 199.2\alpha^2 - 39.7\alpha^3 , \quad \text{for } 0.5 \leq \alpha \leq 3.0 \tag{69}$$

Though Eqs. 66, 67, 68 and 69 are of the same type, an attempt to establish the function $\gamma^* = f(\alpha,\eta)$ was not successful. For comparison, the approximate equations have been plotted with the calculated curves as shown in Figs. 8, 9, 10 and 11.

VI. CONCLUSIONS

With the investigation limited in scope to the case of a simply supported plate stiffened by one longitudinal stiffener, the following conclusions can be drawn:

(1) The Rayleigh-Ritz method can be used to analyze the buckling of stiffened plates with good accuracy if enough coefficients of the assumed series are used.

(2) From Table 2, it can be concluded that the limiting buckling values (upper limits) calculated from Eqs. 2 and 3 are not all conservative compared to those values determined using the Rayleigh-Ritz method.

(3) The limiting buckling values are not the maximum buckling coefficients attainable.

(4) If the aspect ratio α of the plate is constant, the minimum rigidity ratio γ^* increases as the position parameter η increases.

VII. RECOMMENDATIONS FOR FURTHER STUDY

The following are recommended as subjects for further investigation.

(1) Determine the minimum stiffener rigidity ratio γ^* for cases of more than one longitudinal stiffener and of longitudinal and transverse stiffeners crossing each other orthogonally under all kinds of stress boundary conditions.

(2) Investigate the possibility of obtaining the equation

$$\gamma^* = f(\alpha, \eta)$$

in which α is the aspect ratio of the plate and η is the location parameter of the stiffener, for each case.

(3) As the limiting buckling values are not the maximum buckling values attainable, using larger buckling matrices to investigate the behavior of the plate beyond the limiting buckling values is recommended.

(4) Find γ^* based on the maximum buckling values, provided the maximum buckling values have been determined as indicated in the above recommendation.

VIII. ACKNOWLEDGEMENTS

The author expresses his sincere appreciation to Dr. Peter B. Cooper, Associate Professor of Civil Engineering at Kansas State University, for his guidance in the research and constant encouragement during the writing of this thesis. Thanks are also extended to Dr. Jack B. Blackburn, Head of Civil Engineering Department, Professor V. H. Rosebraugh and Dr. C. L. Huang for serving on the advisory committee.

Appreciation is also extended to the 360 IBM Computing Center of Kansas State University. Without its facilities for high-speed computation, most calculations of this research would have been impossible.

REFERENCES

1. Klöppel, K. and Scheer, J., BEULWERTE AUSGESTEIFTER RECHTECKPLATTEN, Verlag von Wilhelm Ernst & Sohn, Berlin, 1960.

2. Timoshenko, S. P., HISTORY OF STRENGTH OF MATERIALS, McGraw-Hill, 1953, chapt. IV, V, VIII.

3. Timoshenko, S. P. and Gere, J. M., THEORY OF ELASTIC STABILITY, McGraw-Hill, 1961, chapt. 8,9.

4. Cooper, P. B., LITERATURE SURVEY ON LONGITUDINALLY STIFFENED PLATES, Lehigh University Institute of Research, 1963.

5. Timoshenko, S. P. ÜBER DIE STABILITAT VERSTEIFTER PLATTEN, Eisenbau, Vol. 12, 1921, p. 147.

6. Southwell, R. V. and Skan, S.W., ON THE STABILITY UNDER SHEARING FORCES OF A FLAT ELASTIC STRIP, Proceedings of the Royal Society, London, Eng., Vol. 105, series A, 1924.

7. Bergmann, S. and Reissner, H., BUCKLING OF CORRUGATED STRIPS SUBJECTED TO SHEAR STRESSES, Zeitschrift fur Flugtechnik und Motorluftschiffahrt, vol. 20, 1929, p. 475; vol. 21, 1930, p. 306.

8. Schmieden, C., BUCKLING OF STIFFENED PLATES IN SHEAR, Zeitschrift fur Flugtechnik und Motorluftschiffahrt, vol. 21, 1930, p. 61.

9. Huber, M. T., THE THEORY OF CROSSWISE REINFORCED CONCRETE STEEL PLATES WITH APPLICATIONS TO VARIOUS STRUCTURALLY IMPORTANT PROBLEMS ON RECTANGULAR PLATES, Bauingenieur, 1923, nos. 12-13, p. 354.

10. Seydel, E., BEITRAG ZUR FRAGE DES AUSBEULENS VON VERSTEISTEN PLATTEN BEI SCHUBBEANSPRUCHUNG, Jahrbuch 1930 der dertschen Versuchsanstalt fur Luftfahrt e.V., Berlin-Adlershof-Verlag von R. Oldenbourg, Munich, Berlin, 1930, pp. 235-254.

11. Wang, T. K., BUCKLING OF TRANSVERSE STIFFENED PLATES UNDER SHEAR, J. Appl. Mech., vol. 14, p. 269, 1947.

12. Klöppel, K. and Scheer, J., BEULWERTE DER DURCH ZWEI GLEICHE LANGSSTEIFEN IN DEN DRITTELSPUNKTEN DER FELDBREITE AUSGESTEIFTEN RECHTECKPLATTE BEI NAVIERSCHEN RANDBEDINGUNGEN, Stahlbau, vol. 25, 1956 a and vol. 26, 1957, p. 246.

13. Kloppel, K. and Scheer, J., BEULWERTE DER DURCH EINE LANGSSTEIFE IM DRITTELSPUNKT DER FELDBREITE ASUGESTEIFTEN RECHTECKPLATTE BEI NAIERSCHEN, Stahlbau, vol. 26, 1957, p. 364.

14. Scott, M. and Weber, R. L., REQUIREMENTS FOR AUXILIARY STIFFENERS ATTACHED TO PANELS UNDER COMBINED COMPRESSION AND SHEAR, N.A.C. A.T.N. 921, December, 1942.

15. Moore, R. L., AN INVESTIGATION OF THE EFFECTIVENESS OF STIFFENERS ON SHEAR-RESISTANT PLATE GIRDER WEBS, N.A.C.A.T.N. No. 862, September, 1942.

16. Bleich, F., BUCKLING STRENGTH OF METAL STRUCTURES, McGraw-Hill, 1952.

17. Wang, C. T., APPLIED ELASTICITY, McGraw-Hill, 1953.

18. Kuo, Shan S., NUMERICAL METHODS AND COMPUTERS, Addison-Wesley Publishing Company, 1965.

19. Crandall, Stephen H., ENGINEERING ANALYSIS

20. Wylie, Clarence R., ADVANCED ENGINEERING MATHEMATICS, 2nd. ed. New York, McGraw-Hill, 1960.

21. Borsch-Supan, W.: BERECHNUNG VON BEULWERTEN VERSTEIFTER PLATTEN AUF RECHENAUTOMATEN: MATHEMATISCHE GRUNDLAGEN UND PRAKTISCHES VORGEHEN. Stahlbau, vol. 28, 1959, p. 37.

22. Borsch-Supan, W.: BEULSICHERHEIT AUSGESTEIFTER RECHTECKPLATTEN BEI ZUSAMMENGESETZTER BEANSPRUCHUNG, Stahlbau, vol. 28, 1959, p. 68.

TABLES AND FIGURES

Table 1. Buckling coefficients for unstiffened plate

α_μ	k_μ Values		Corresponding Stiffened Plate	
	By Formula*	Calculated**	η	α
0.63	17.45	17.716	0.2	0.50
0.71	14.60	14.310	0.3	0.50
0.83	11.24	11.518	0.4	0.50
1.00	9.34	9.343	0.5	0.50
0.93	10.17	9.999	0.2	0.75
1.07	8.84	8.753	0.3	0.75
1.25	7.90	7.781	0.4	0.75
1.50	7.12	7.083	0.5	0.75
1.25	7.90	7.781	0.2	1.00
1.43	7.29	7.232	0.3	1.00
1.67	6.78	6.834	0.4	1.00
2.00	6.34	6.561	0.5	1.00
1.56	6.98	6.976	0.2	1.25
1.79	6.59	6.713	0.3	1.25
2.08	6.26	6.481	0.4	1.25
2.50	5.96	6.069	0.5	1.25
1.88	6.47	6.643	0.2	1.50
2.14	6.21	6.401	0.3	1.50
2.50	5.96	6.069	0.4	1.50
3.00	5.78	5.863	0.5	1.50
2.50	5.96	6.069	0.2	2.00
2.86	5.83	5.903	0.3	2.00
3.33	5.71	5.801	0.4	2.00
4.00	5.59	5.640	0.5	2.00

Table 1. (Continued)

α_μ	k_μ Values		Corresponding Stiffened Plate	
	By Formulas*	Calculated**	η	α
3.13	5.75	5.824	0.2	2.50
3.57	5.65	5.724	0.3	2.50
4.17	5.57	5.616	0.4	2.50
5.00	5.500	5.552	0.5	2.50
3.75	5.62	5.679	0.2	3.00
4.29	5.56	5.605	0.3	3.00
5.00	5.500	5.552	0.4	3.00
6.00	5.451	5.493	0.5	3.00

*Calculated by formulas:

$$k_\mu = 4.00 + 5.34/\alpha_\mu^2, \quad \text{for } \alpha \leq 1 \tag{63}$$

$$k_\mu = 5.34 + 4.00/\alpha_\mu^2, \quad \text{for } \alpha \geq 1 \tag{64}$$

**Calculated in this research by Rayleigh-Ritz Method.

Table 2. Limiting Buckling Values k_{max}

η	α	0.50	0.75	1.00	1.25	1.50	2.00	2.50	3.00
0.2	I	27.681	15.624	12.158	10.900	10.379	9.453	9.101	8.874
	II	27.610	15.743	12.344	10.904	10.122	9.344	8.984	8.788
0.3	I	29.205	17.865	14.760	13.701	13.063	12.020	11.682	11.440
	II	29.523	18.009	14.898	13.458	12.676	11.898	11.538	11.342
0.4	I	31.995	21.615	18.984	18.004	16.860	16.055	15.599	15.422
	II	32.471	21.944	18.833	17.393	16.611	15.833	15.473	15.278
0.5	I	37.370	28.333	26.242	24.278	23.451	22.560	22.207	21.973
	II	37.360	28.471	25.360	23.920	23.138	22.360	22.000	21.804

I. Calculated in this research by Rayleigh-Ritz Method.

II. Calculated by following formulas:

$$k_{max} = \{4.00 + 5.34/[\alpha/(1-\eta)^2]^2\}/(1-\eta)^2, \quad \text{for } \alpha/1-\eta \leq 1 \tag{2}$$

$$k_{max} = \{5.34 + 4.00/[\alpha/(1-\eta)^2]^2\}/(1-\eta)^2, \quad \text{for } \alpha/1-\eta \geq 1 \tag{3}$$

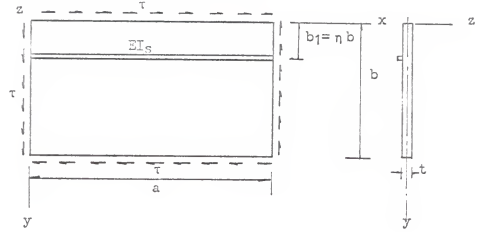

Fig. 1. Notation of the Plate

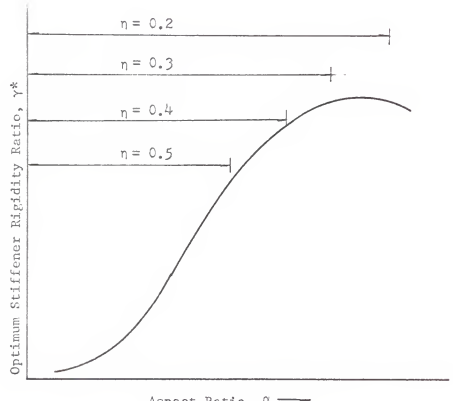

Fig. 2. Typical Form of γ^* vs. α Curves

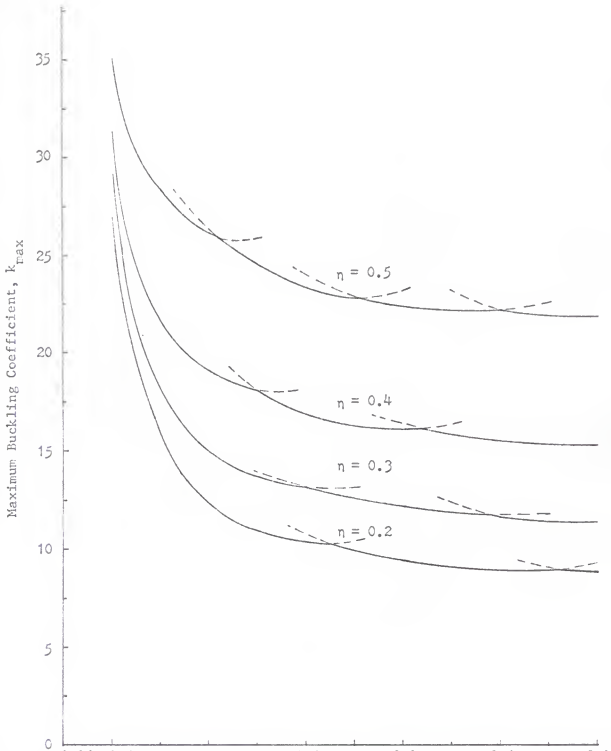

Fig. 3. Limiting Buckling Values k_{max}

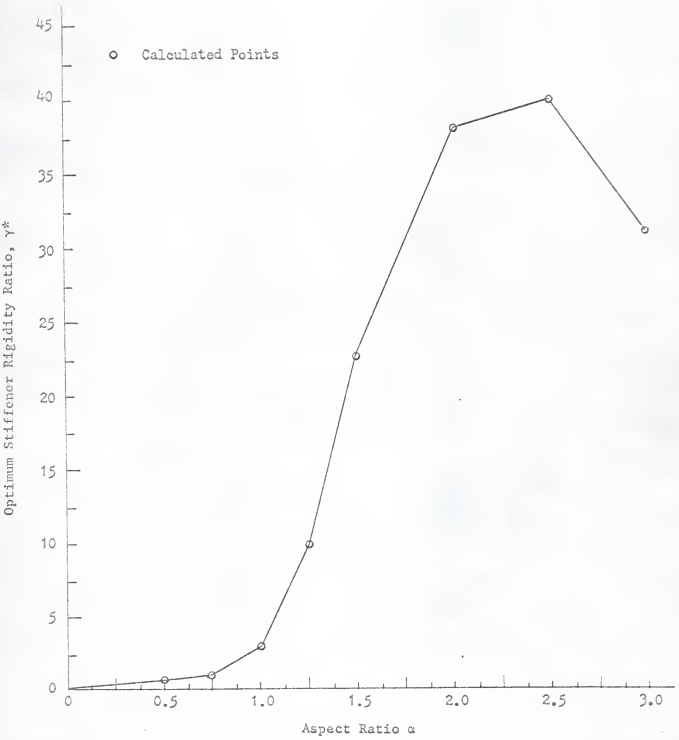

Fig. 4. Minimum Stiffener Rigidity Ratio vs. Aspect Ratio for $\eta = 0.2$

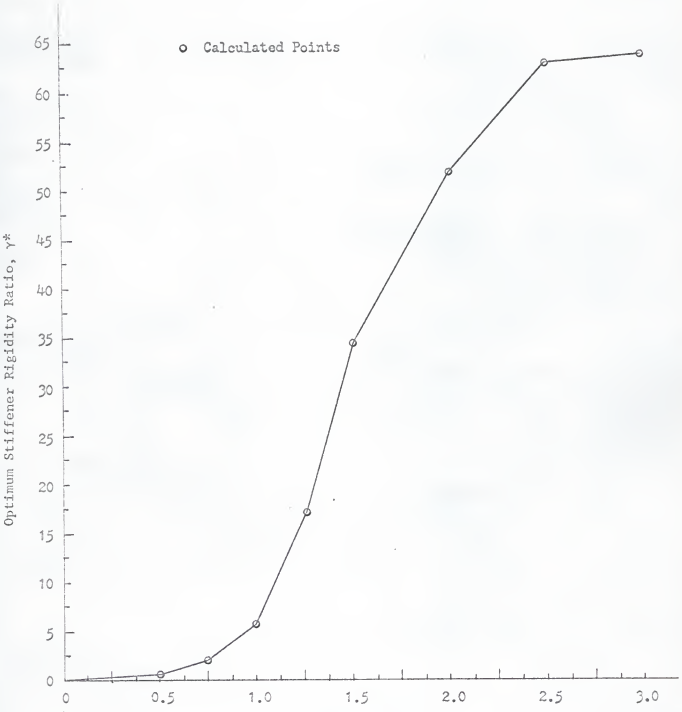

Fig. 5. Minimum Stiffener Rigidity Ratio vs. Aspect Ratio for n = 0.3

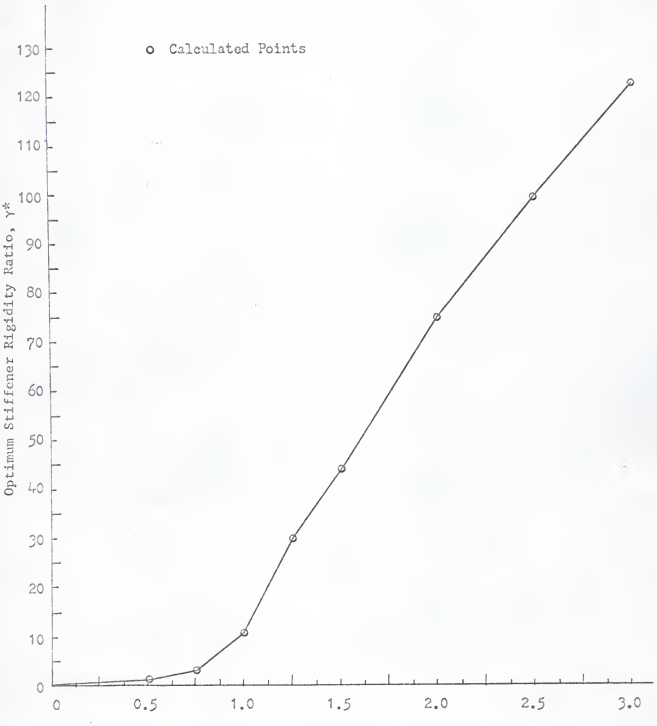

Fig. 6. Minimum Stiffener Rigidity Ratio vs. Aspect Ratio for $\eta = 0.4$

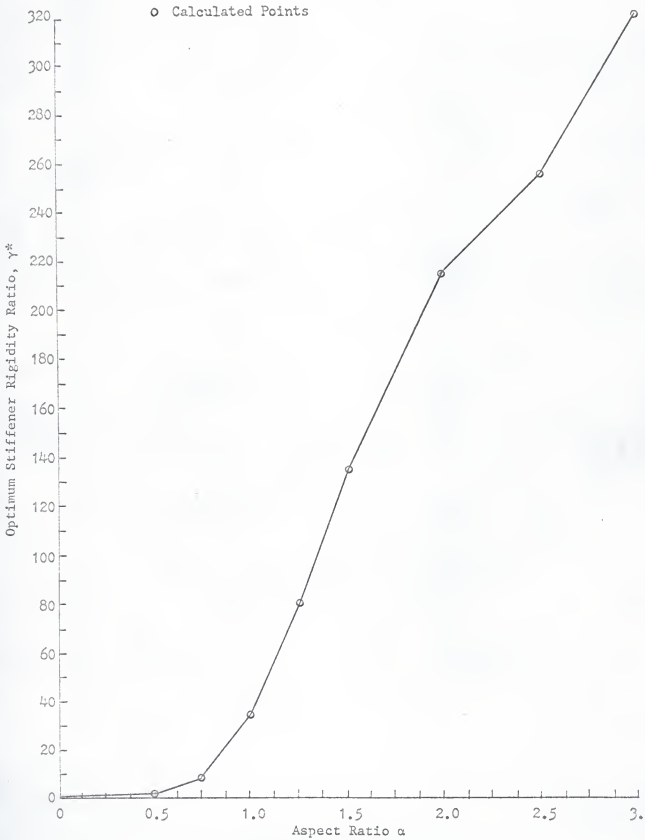

Fig. 7. Minimum Stiffener Rigidity Ratio vs. Aspect Ratio for $\eta = 0.5$

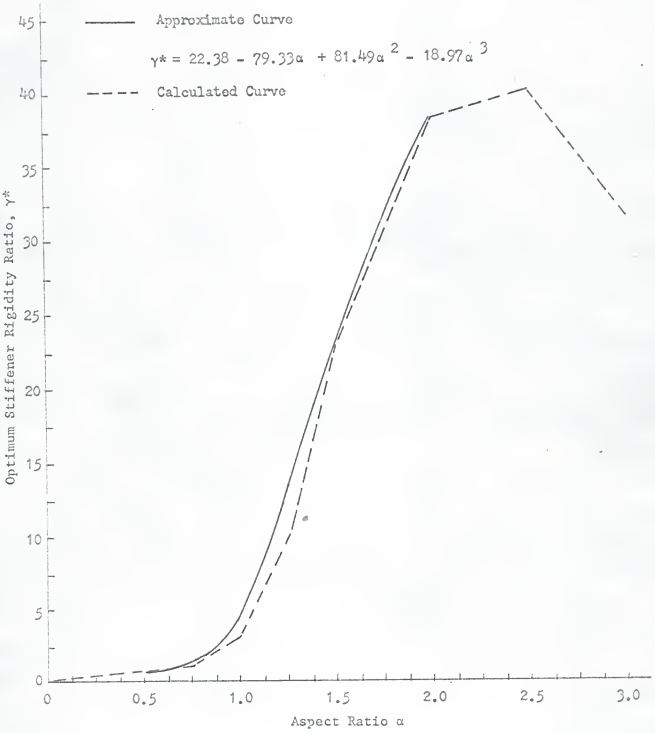

Fig. 8. Comparison of Approximate and Calculated Curves for $\eta = 0.2$

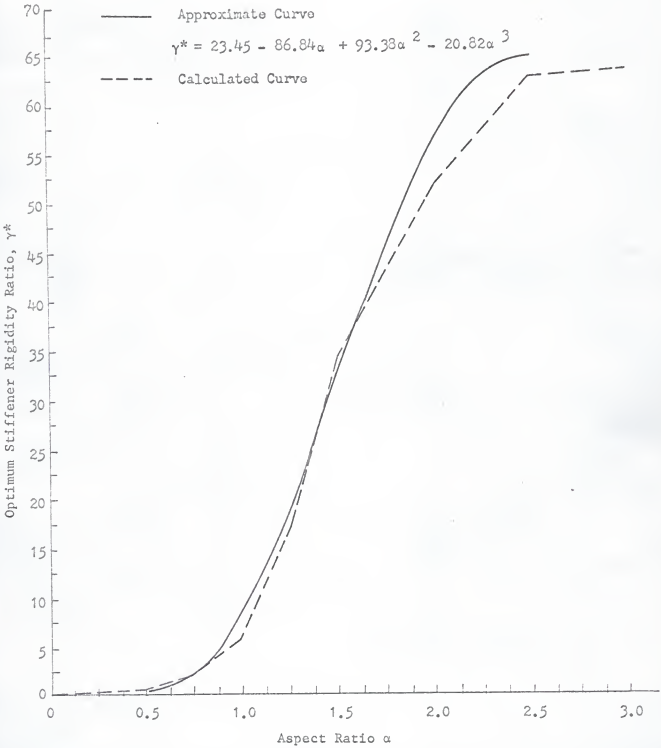

Fig. 9. Comparison of Approximate and Calculated Curves for $\eta = 0.3$

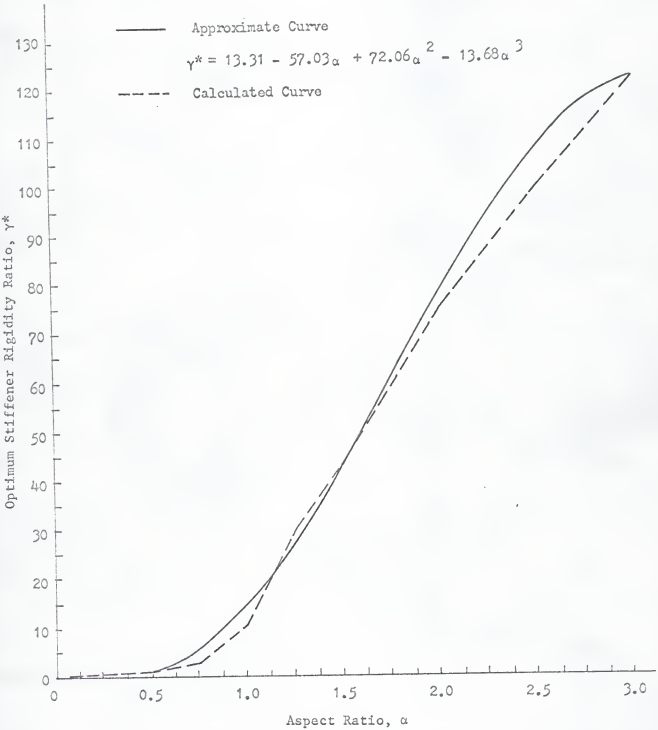

Fig. 10. Comparison of Approximate and Calculated Curves for $\eta = 0.4$

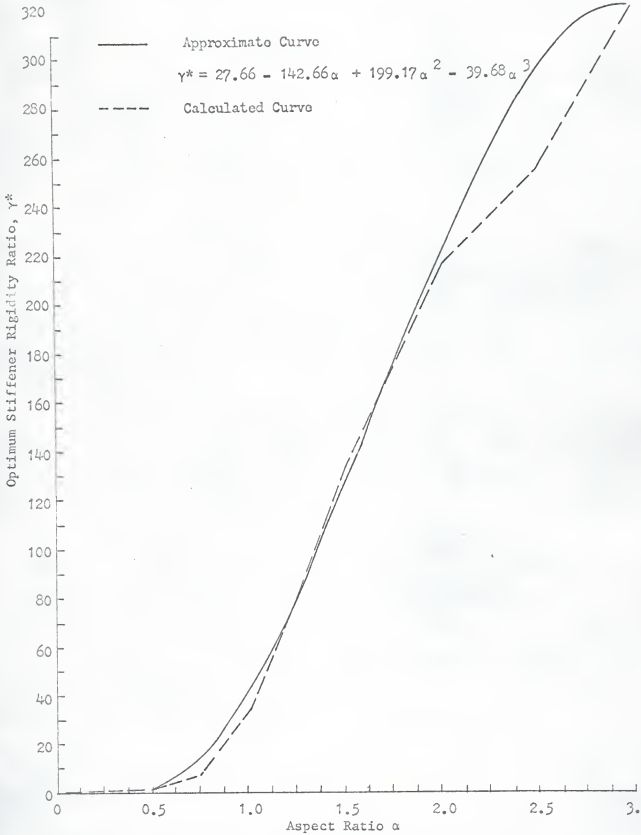

Fig. 11. Comparison of Approximate and Calculated Curves for $\eta = 0.5$

NOTATION

a = length of plate

b = width of plate

$D = Et^3/12(1-\mu^2)$, flexural rigidity of plate

E = modulus of elasticity

I_s = moment of inertia of stiffener

τ = shear in pounds per square inch

τ_{cr} = critical shearing stress in pounds per square inch

t = thickness of plate

$\alpha = a/b$, aspect ratio of plate

$\beta = b/t$, slenderness of plate

b_1 = location of stiffener from x-axis

$\eta = b_1/b$, stiffener location parameter

$\gamma_L = EI_s/bD$, stiffener rigidity ratio

μ = Poisson's ratio

W = deflection of plate in z direction

A_{mn} = coefficient of double Fourier series

U_p = internal energy of plate

U_s = internal energy of stiffener

W = external energy of plate

$\Pi = U_p + U_s - W$, total potential energy of the system

$[M]$ = buckling matrix

$[A],[B]$ = submatrices of $[M]$

$\sigma_e = \pi^2 Et^2/12b^2(1-\mu^2)$

$C = 4\alpha^3/t\pi^2\sigma_e = 4a^3/b\pi^4 D$

$R_{mn} = (m^2 + \alpha^2 n^2)^2$

$S_m = 2m^4 \gamma_L$

$T = 32\alpha^3/\pi^2$

m,n,p,q = integers, number or subscripts

α_μ = aspect ratio for unstiffened plate

k = buckling coefficient of stiffened plate

k_u = buckling coefficient of unstiffened plate

γ^* = least required rigidity ratio

k_{max} = upper limit of buckling coefficient of stiffened plate

APPENDIX I

FLOW DIAGRAM FOR SOLUTION OF BUCKLING COEFFICIENT

The following symbols are used in the flow diagram:

A, B = matrices of Eq. 38.

am, an = number of components of the assumed series in x and y directions, respectively.

N = order of matrices A and B

k = smallest eigenvalue of Eq. 38, also the buckling coefficient.

α = aspect ratio of the plate

γ_L = stiffener rigidity ratio

η = location of the stiffener

The arguments used in the subroutine JACOBI are defined as follows:

N = order of the given real symmetric matrix [Q]

Q = the matrix [Q] to be diagonalized (This input matrix is later destroyed)

M = the number of rotations performed

V = storage for eigenvectors

(1). Main Program 1

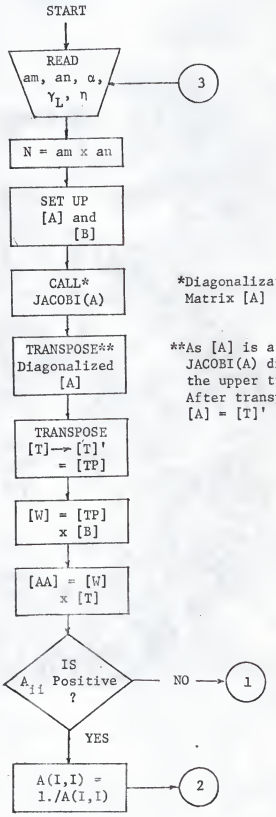

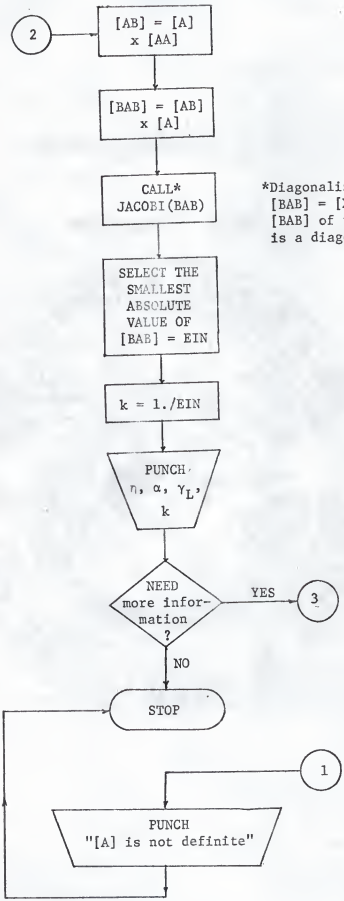
2
[AB] = [A] x [AA]
[BAB] = [AB] x [A]
CALL* JACOBI(BAB)
*Diagonalize [BAB]
[BAB] = [XX]' [BAB][XX]
[BAB] of right hand side is a diagonalized matrix
SELECT THE SMALLEST ABSOLUTE VALUE OF [BAB] = EIN
k = 1./EIN
PUNCH η, α, γL, k
NEED more information ?
YES
3
NO
STOP
1
PUNCH "[A] is not definite"

(2). Main Program 2 - Set up matrix [A]

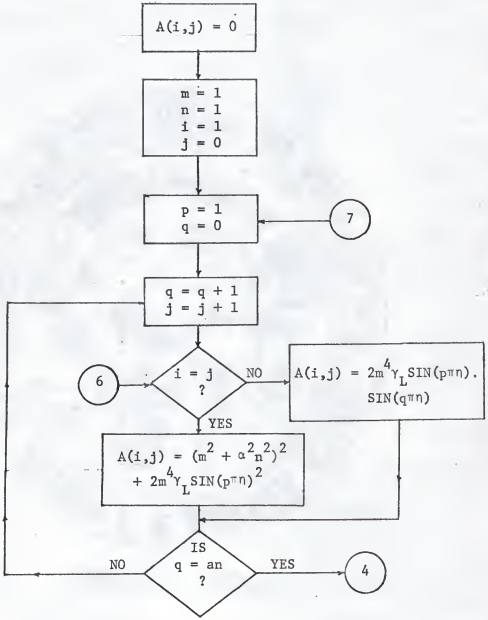

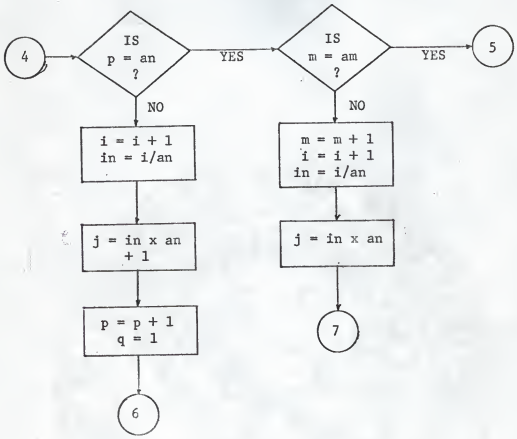
4
IS
p = an
?
YES
IS
m = am
?
YES
5
NO
NO
i = i + 1
in = i/an
m = m + 1
i = i + 1
in = i/an
j = in x an
+ 1
j = in x an
p = p + 1
q = 1
7
6

(3). Main Program 3 - Set up matrix [B]

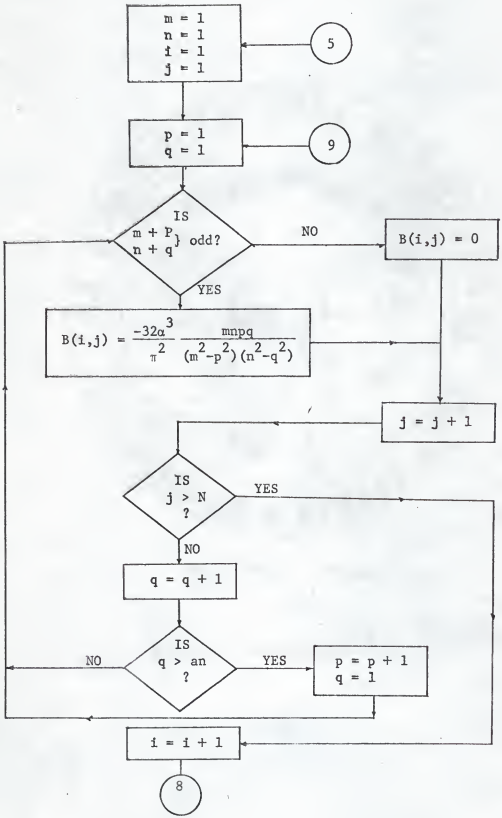

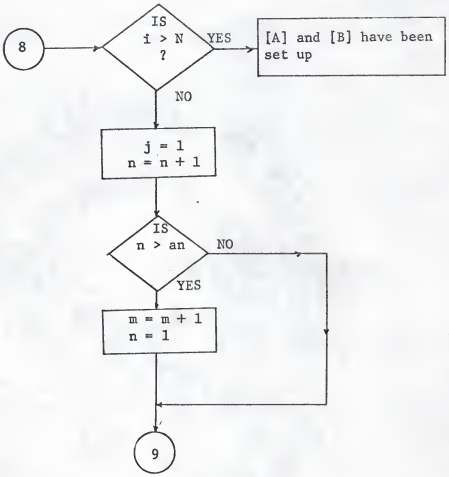
8
IS
i > N
?
YES
[A] and [B] have been set up
NO
j = 1
n = n + 1
IS
n > an
NO
YES
m = m + 1
n = 1
9

(4). Subroutine - JACOBI

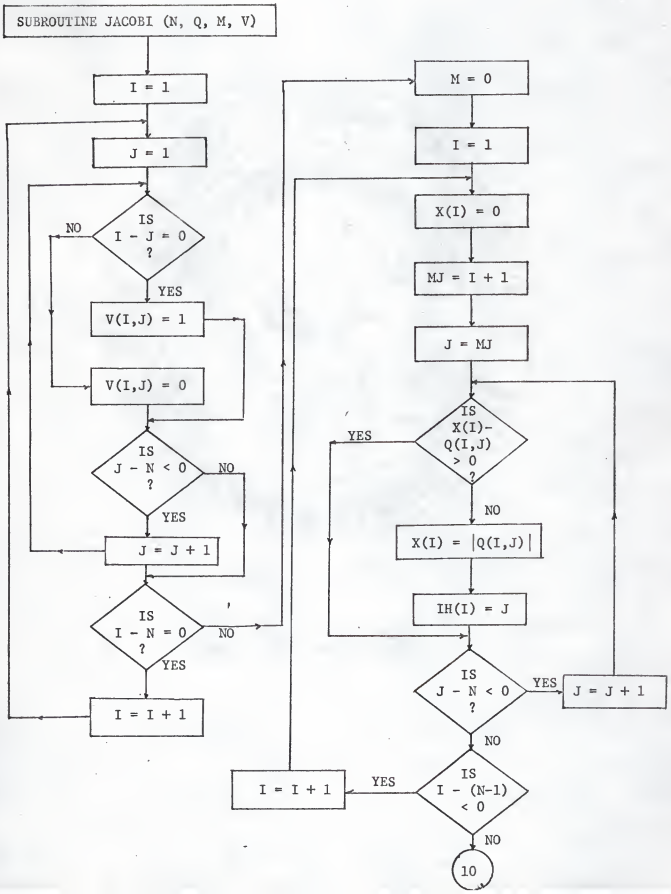

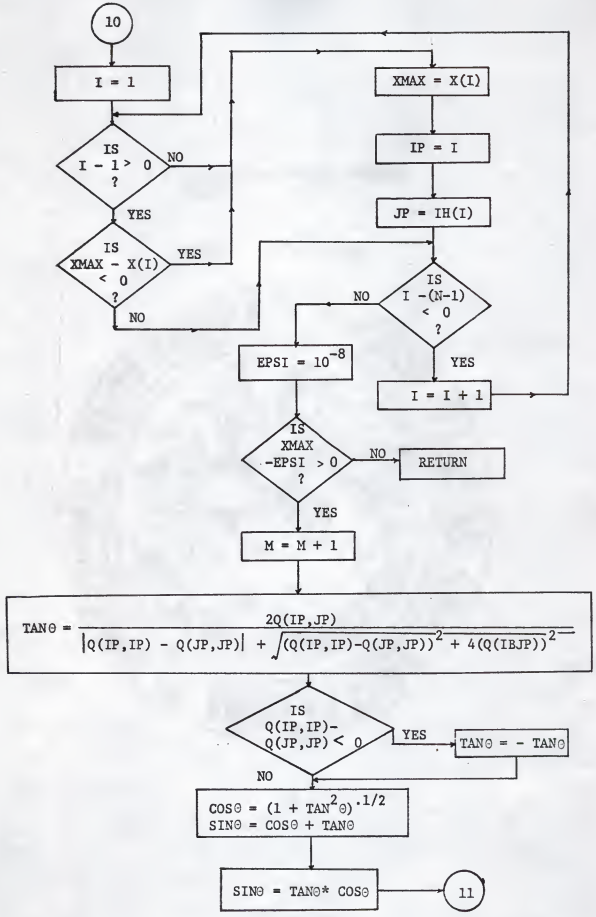
10
I = 1
IS I - 1 > 0 ?
NO
YES
IS XMAX - X(I) < 0 ?
YES
NO
XMAX = X(I)
IP = I
JP = IH(I)
IS I -(N-1) < 0 ?
NO
YES
I = I + 1
EPSI = 10^-8
IS XMAX -EPSI > 0 ?
NO
RETURN
YES
M = M + 1
TANΘ = 2Q(IP,JP) / |Q(IP,IP) - Q(JP,JP)| + √((Q(IP,IP)-Q(JP,JP))^2 + 4(Q(IBJP))^2)
IS Q(IP,IP)- Q(JP,JP) < 0
YES
TANΘ = - TANΘ
NO
COSΘ = (1 + TAN^2Θ)·1/2
SINΘ = COSΘ + TANΘ
SINΘ = TANΘ* COSΘ
11

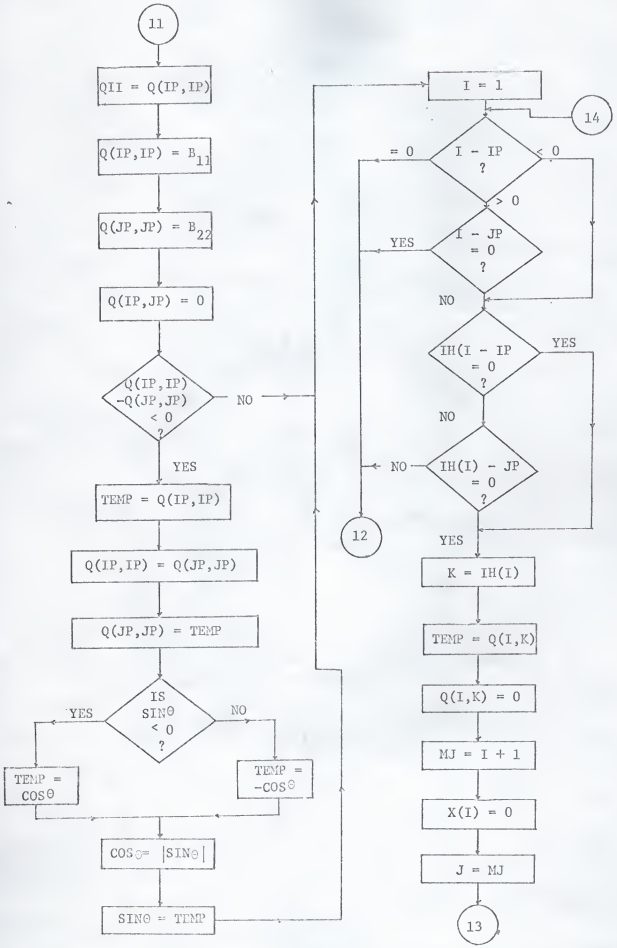
11
QII = Q(IP,IP)
Q(IP,IP) = B11
Q(JP,JP) = B22
Q(IP,JP) = 0
Q(IP,IP) -Q(JP,JP) < 0 ?
NO
YES
TEMP = Q(IP,IP)
Q(IP,IP) = Q(JP,JP)
Q(JP,JP) = TEMP
IS SINΘ < 0 ?
YES
NO
TEMP = COSΘ
TEMP = -COSΘ
COSΘ = |SINΘ|
SINΘ = TEMP
I = 1
14
I - IP ?
= 0
< 0
> 0
I - JP = 0 ?
YES
NO
IH(I - IP = 0 ?
YES
NO
IH(I) - JP = 0 ?
NO
YES
12
K = IH(I)
TEMP = Q(I,K)
Q(I,K) = 0
MJ = I + 1
X(I) = 0
J = MJ
13

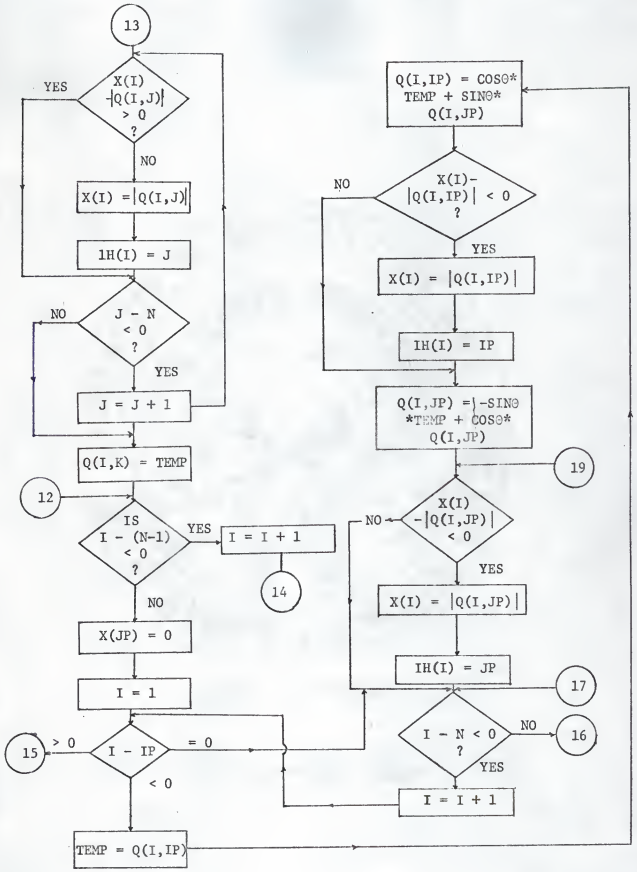
13
X(I) -|Q(I,J)| > 0 ?
YES
NO
X(I) = |Q(I,J)|
1H(I) = J
J - N < 0 ?
NO
YES
J = J + 1
Q(I,K) = TEMP
12
IS I - (N-1) < 0 ?
YES
I = I + 1
14
NO
X(JP) = 0
I = 1
15
I - IP
> 0
= 0
< 0
TEMP = Q(I,IP)
Q(I,IP) = COSΘ* TEMP + SINΘ* Q(I,JP)
X(I) -|Q(I,IP)| < 0 ?
NO
YES
X(I) = |Q(I,IP)|
IH(I) = IP
Q(I,JP) =|-SINΘ *TEMP + COSΘ* Q(I,JP)
19
X(I) -|Q(I,JP)| < 0
NO
YES
X(I) = |Q(I,JP)|
IH(I) = JP
17
I - N < 0 ?
NO
16
YES
I = I + 1

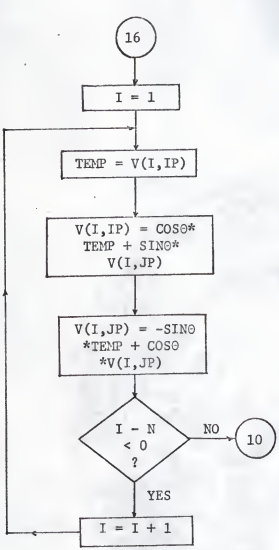
16
I = 1
TEMP = V(I,IP)
V(I,IP) = COSΘ*
TEMP + SINΘ*
V(I,JP)
V(I,JP) = -SINΘ
*TEMP + COSΘ
*V(I,JP)
I - N
< 0
?
NO
10
YES
I = I + 1

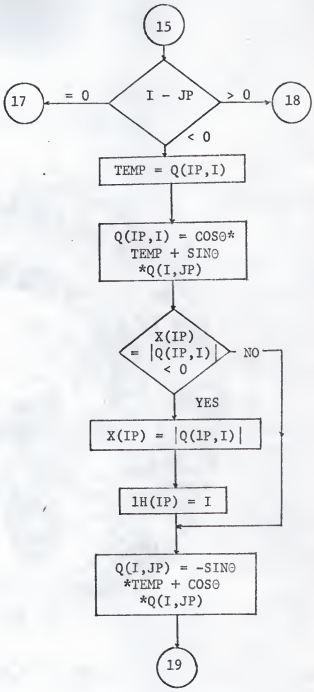
15
I - JP
= 0
> 0
< 0
17
18
TEMP = Q(IP,I)
Q(IP,I) = COSΘ*
TEMP + SINΘ
*Q(I,JP)
X(IP)
= |Q(IP,I)|
< 0
NO
YES
X(IP) = |Q(IP,I)|
IH(IP) = I
Q(I,JP) = -SINΘ
*TEMP + COSΘ
*Q(I,JP)
19

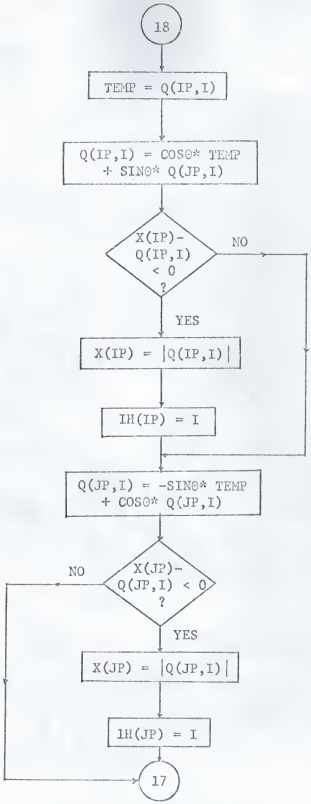
18
TEMP = Q(IP,I)
Q(IP,I) = COSΘ* TEMP + SINΘ* Q(JP,I)
X(IP)- Q(IP,I) < 0 ?
NO
YES
X(IP) = |Q(IP,I)|
IH(IP) = I
Q(JP,I) = -SINΘ* TEMP + COSΘ* Q(JP,I)
X(JP)- Q(JP,I) < 0 ?
NO
YES
X(JP) = |Q(JP,I)|
IH(JP) = I
17

APPENDIX II

FLOW DIAGRAM FOR POLYNOMIAL INTERPOLATION OF BUCKLING COEFFICIENT

The following symbols are used in the flow diagram:

N = number of known buckling coefficients

NN = number of buckling coefficients to be calculated

x( ) = α values (aspect ratio of the plate) of NN buckling coefficients.

Zx( ) = α values of known buckling coefficients

Y( ) = known buckling coefficients corresponding to Zx( )

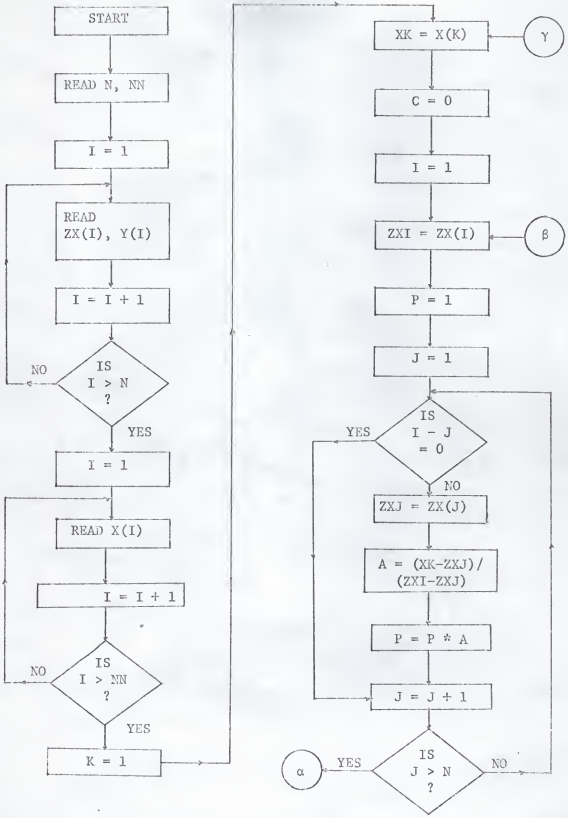
START
READ N, NN
I = 1
READ ZX(I), Y(I)
I = I + 1
IS I > N ?
NO
YES
I = 1
READ X(I)
I = I + 1
IS I > NN ?
NO
YES
K = 1
XK = X(K)
γ
C = 0
I = 1
ZXI = ZX(I)
β
P = 1
J = 1
IS I - J = 0
YES
NO
ZXJ = ZX(J)
A = (XK-ZXJ)/(ZXI-ZXJ)
P = P * A
J = J + 1
IS J > N ?
α
YES
NO

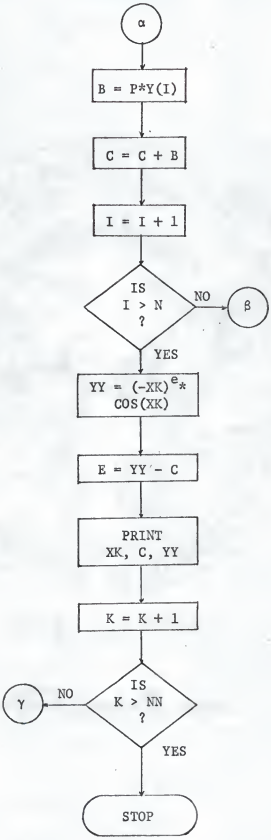
α
B = P*Y(I)
C = C + B
I = I + 1
IS I > N ?
NO
β
YES
YY = (-XK)^e * COS(XK)
E = YY - C
PRINT XK, C, YY
K = K + 1
IS K > NN ?
NO
γ
YES
STOP

ELASTIC BUCKLING OF LONGITUDINALLY STIFFENED PLATES UNDER SHEAR

by

KANG-SHYONG LIU

Diploma, Taipei Institute of Technology, 1962

AN ABSTRACT OF A MASTER'S THESIS

submitted in partial fulfillment of the

requirements for the degree

MASTER OF SCIENCE

Department of Civil Engineering

KANSAS STATE UNIVERSITY

Manhattan, Kansas

1969

ABSTRACT

This thesis presents an analysis of the elastic buckling of a simply supported rectangular plate reinforced by a single longitudinal stiffener and subjected to uniformly distributed shearing stresses along the four edges. The variables considered in the analysis were the plate aspect ratio (width-to-depth ratio), the longitudinal stiffener position and the rigidity of the stiffener. The purpose of the investigation was to determine the optimum stiffener rigidity for various stiffener positions and aspect ratios.

The Rayleigh-Ritz energy method was used in this research to derive the governing matrix equation, which in turn was programmed for computer solution using the successive rotation method of analysis.

The results are presented in the form of optimum rigidity ratio versus aspect ratio curves. For design purposes, approximate formulas for these curves were determined by curve fitting procedures.